Neoplasma 2024; 71(5): 428–441

doi:10.4149/neo_2024_240502N196

EIF4A3-induced circle RNA_ 0001860 promotes growth, invasion, and immune evasion of gastric cancer cells through the miR-618/HMGA2 axis

Xiaoyi ZHANG[1], Jiaqi LI[2], Qian ZHANG[2,*]

[1]*The First Cardiovascular Department, The Third Affiliated Hospital of Heilongjiang University of Chinese Medicine, Heilongjiang, China;* [2]*Department of Abdominal Radiotherapy, Harbin Medical University Cancer Hospital, Heilongjiang, China*

**Correspondence: zhangqianhmu@21cn.com*

Received May 2, 2024 / Accepted October 10, 2024

Gastric cancer is a globally common type of cancer with a dismal prognosis. Circle RNA_ 0001860 (circ_0001860) is dysregulated in several cancers and involved in cancer development. Its involvement in stomach cancer, however, remains unclear. AGS and HGC-27 cells were transfected with shRNA against circ_0001860 to knock down the circ_0001860 level. The function of circ_0001860 in gastric cancer was analyzed by cell counting kit-8, 5-ethynyl-2'-deoxyuridine (EdU) incorporation, Transwell, ELISA, dual-luciferase reporter, RIP, RNA pull-down, and western blotting. Nude mice were subcutaneously inoculated with AGS cells with lentivirus-packaged sh-circ_0001860 to determine the role of sh-circ_0001860 in gastric cancer by immunohistochemistry assays. circ_0001860 was upregulated in gastric cancer, indicating a poor prognosis for gastric cancer patients. Knockdown of circ_0001860 reduced gastric cancer cells' viability, the percentage of EdU-positive cells, the numbers of invaded cells, and concentrations of IL-10 and TGF-β while fostering the concentrations of IFN-γ and IL-2. circ_0001860 sponged miR-618 to positively modulate the HMGA2 level in gastric cancer cells. The inhibitory role of sh-circ_0001860 on cell growth, invasion, and immune evasion of gastric cancer was abolished with the miR-618 knockdown or the HMGA2 overexpression. Besides, EIF4A3 positively modulated the circ_0001860 level in gastric cancer cells. In vivo, silencing of circ_0001860 reduced tumor size and weight and the expression of HMGA2 and IL-10 but enhanced the level of miR-618 and IFN-γ. Collectively, circle RNA_ 0001860 was induced by EIF4A3 to enhance proliferation, invasion, and immune evasion of gastric cancer through the miR-618/HMGA2 axis.

Key words: gastric cancer; circ_0001860; miR-618; HMGA2; EIF4A3; invasion; immune escape

As one of the most frequent cancers of the digestive tract, gastric cancer is also the most prevalent type of cancer overall and the third leading cause of cancer-related fatalities, affecting approximately one million individuals each year [1]. This malignancy has been associated with a number of established risk factors, including *Helicobacter pylori* infection, particular genetic variations, smoking, and eating habits [2]. Surgical excision is the main treatment for gastric cancer, which is often combined with chemotherapy or radiation [3]. Novel therapeutic approaches, such as immunotherapies and targeted medicines, are presently under investigation and may enhance patient results [4]. There has been a decrease in both the incidence and mortality of stomach cancer over the last several decades as a result of advancements in screening, prevention, and therapy. Nonetheless, the prognosis for those with advanced gastric cancer is still not good [5]. Patients with gastric cancer in stage II have a 5-year survival rate of 61–63%, while those in stage III have a 5-year survival rate of roughly 30–35% [6]. Additionally, about 80% of Chinese patients with gastric cancer had advanced or locally progressed disease at the time of diagnosis, which resulted in a poor prognosis and cancer-related death, placing a significant strain on patients and the community [7]. Therefore, in order to assist the clinical advancement of gastric cancer diagnosis and treatment, it is essential to investigate potential novel targets for the disease.

Circular RNAs (circRNAs) are a category of noncoding RNAs (ncRNAs) that are essential in the development of several disease models, including cancer [8], cardiovascular disorders [9], neurological conditions [10], and autoimmune diseases [11]. Numerous studies have consistently shown that circRNAs contribute significantly to gastric cancer via sponging miRNAs. For instance, circNRD1 sequesters microRNA-421 to prevent growth and tumorigenesis

by upregulating THAP11 in gastric cancer [12]. circGLIS3 upregulates PGK1 by sponge miR-1343-3p to enhance cell growth, mobility, and invasion of gastric cancer [13]. circ1811 regulates the malignant progress of gastric cancer cells, including growth, migration, invasion, and apoptosis, through the miR-632/DAPK1 axis [14]. circ_0001860 (circRNA-7), located on chromosome 9, is proven to be downregulated in medroxyprogesterone acetate-resistant cells and tissue, and the knockdown of circ_0001860 accelerates growth and suppresses apoptosis and medroxyprogesterone acetate sensitivity via miR-520h/Smad7 axis in endometrial cancer [15]. Nevertheless, the role and potential mechanism of circ_0001860 in gastric cancer remain undiscovered.

Therefore, the purpose of this study was to discuss the function and potential mechanism of circ_0001860 in the development of gastric cancer. We hope our findings can lay a theoretical basis for the identification and management of gastric cancer.

Patients and methods

Tissue specimen. Patients with gastric cancer who were diagnosed and treated at our hospital had their gastric cancer and the surrounding normal control tissues (n=62) taken. After the patients' tissues were removed, they were immediately frozen in liquid nitrogen and kept at –80 °C until needed. Before surgery, none of the patients accepted immunotherapy, chemotherapy, or preoperative radiation. All the patients have only one form of cancer. Tumor tissues were at least 5 cm apart from the nearby normal tissues. This research was conducted according to the Declaration of Helsinki and permitted by the Board and Ethics Committee of Harbin Medical University Cancer Hospital (approval number: YD2022-06). All participants signed the written informed consent.

Reverse transcription quantitative polymerase chain reaction (RT-qPCR). TRIzol reagent (15596026, Thermo Fisher Scientific, Waltham, MA, USA) was utilized to yield total RNA from gastric cancer tissues or cells. The Bio-Rad ScripTM cDNA Synthesis Kit (1708890, Bio-Rad Laboratories, Inc., Hercules, CA, USA) was then used to execute the RT assay in accordance with the operating manual. RT-qPCR was performed on the Bio-Rad CFX Manager software (Bio-Rad Laboratories, Inc.) with 2× SYBR Master mix (RR820A, Takara, Dalian, China), and the RT-qPCR conditions were 5 min at 94 °C, followed by 40 cycles between 94 °C for 10 s and 60 °C for 50 s, and 72 °C for 50 s. The expression level of circ_0001860 and HMGA2 was calculated by the $2^{-\Delta\Delta CT}$ way with the GAPDH as the control gene. The RT experiment was done using the Bulge-Loop™ miRNA RT-qPCR Primer (RiboBio Co., Ltd., Guangzhou, China) to detect the miR-618 level at 42 °C for 1 h and at 70 °C for 10 min. The miR-618 level was analyzed at 95 °C for 10 min, followed by 40 cycles at 95 °C for 5 s, 56 °C for 15 s, and 70 °C for 15 s with U6 as the control. The primer sequences were: 5'-GCTGGATGCTACTGGGATG-3' (circ_0001860 forward), 5'-TGGGCATAATGAATTTGGCT-3' (circ_0001860 reverse); 5'-GGGCGCCGACATTCAAT-3' (HMGA2 forward), 5'-ACTGCAGTGTCTTCTCCCTTCAA-3' (HMGA2 reverse); 5'-GGTGGTCTCCTCTGACTTCAACA-3' (GAPDH forward), 5'-GTTGCTGTAGCCAAATTCGTTGT-3' (GAPDH reverse); 5'-CGGCGGAAACTCTACTTGTCCTT-3' (miR-618 forward), 5'-ATCCAGTGCAGGGTCCGAGG-3' (miR-618 reverse); and 5'-CTCGCTTCGGCAGCACA-3' (U6 forward), 5'-AACGCTTCACGAATTTGCGT-3' (U6 reverse).

Cell culture. Gastric cancer cells HGC-27 (CL-0107) and AGS (CL-0022), as well as normal human gastric epithelial cell line GES-1, were supplied by Procell (Wuhan, China). HGC-27 and GES-1 cells were cultivated in RPMI-1640 media (PM150110, Procell), and AGS cells were cultured in Ham's F-12 media (PM150810, Procell), with 10% fetal bovine serum (FBS, 164210, Procell) as well as 1% penicillin-streptomycin solution (PB180120, Procell) at 37 °C with 5% CO_2.

Cell treatment. To downregulate the circ_0001860 expression, three short-hairpin RNAs (shRNAs) against circ_0001860 (sh-circ_0001860#1, 2, and 3), as well as the scrambled shRNA (sh-NC) were designed and supplied by GenePharma (Shanghai, China). miR-618 mimic and the relevant control miR-NC were obtained from GenePharma to upregulate the level of miR-618. Anti-miR-618 and anti-NC were designed and provided by GenePharma to downregulate the level of miR-618. shRNAs against EIF4A3 (sh-EIF4A3) and sh-NC were provided by GenePharma to downregulate the level of EIF4A3. The sequences of these shRNAs, mimics, inhibitors, and relevant NC are shown in Supplementary Table S1. Besides, the sequences of HMGA2 (NCBI Reference Sequence: NM_003483.6) or EIF4A3 (NCBI Reference Sequence: NM_014740.4) were inserted into pcDNA vector plasmids and transfected into AGS cells using Lipofectamine 3000 (L3000001, Invitrogen, Carlsbad, CA, USA) to upregulate the expression level of HMGA2 or EIF4A3.

Cell counting kit-8 (CCK-8) assay. AGS and HGC-27 cells with a density of 5×10^3 were plated into 96-well plates. Following a 24-hour incubation at 37 °C and 5% CO_2, 10 µl CCK-8 reagents (CA1210, Solarbio, Beijing, China) were added into each well and incubated for 2 h at 37 °C. A microplate reader from Thermo Fisher Scientific (Waltham, MA, USA) was used to measure the absorbance at 450 nm.

The 5-ethynyl-2'-deoxyuridine (EdU) incorporation assay. After incubating for 2 h at 37 °C with 1 ml of EdU working solution (20 µM), the cells were fixed with immunostaining fix solution (Beyotime, Shanghai, China), treated with 0.3% Triton X-100 (Beyotime), and exposed to the anti-EdU Click reaction solution for half an hour in the dark. Next, cell nuclei were stained with Hoechst 33342 (5 µg/ml, Beyotime). Using a fluorescent microscope (IX71, Olympus,

Tokyo, Japan), the pictures were taken. Five random fields were selected to determine the EdU-positive cell percentage by using ImageJ software (National Institutes of Health, USA).

Transwell assay. AGS and HGC-27 cells were resuspended in the Ham's F-12 media (for AGS cells) or RPMI-1640 media (for HGC-27 cells) without FBS and then plated into the upper compartment of 24-well Transwell plates with a density of 5×10^4 cells/well. The Transwell plates were bought from Corning Company (3422, New York, NY, USA) with an 8-μm pore size and coated with Matrigel (356234, Solarbio). The low compartment was filled with media with 20% FBS. Following a 24-hour incubation at 37 °C and 5% CO_2, Matrigel was abraded. The cells were photographed using an Olympus microscope after being fixed with 4% paraformaldehyde (P0099, Beyotime) and stained with 0.1% crystal violet (C0121, Beyotime). The number of invasion cells was counted in five randomly selected fields.

Enzyme-linked immunosorbent assay (ELISA). Using the Human Peripheral Blood Lymphocyte Separation Medium (C0025, Beyotime), peripheral blood mononuclear cells (PBMCs) were collected from whole blood according to the operating manual. The two gastric cancer cell lines were cultured with PBMCs for twenty-four hours after being plated into 24-well plates at a density of 2.5×10^5 cells/well. The contents of interferon-γ (IFN-γ) and interleukin-2 (IL-2), IL-10 and transforming growth factor-β (TGF-β) in the media of co-culture cells were measured with Human IFN-γ ELISA Kit (#PI511, Beyotime), Human IL-2 ELISA Kit (#PI580, Beyotime), Human IL-10 ELISA Kit (#PI528, Beyotime), and Human TGF-β1 ELISA Kit (#PT880, Beyotime) following the operating manuals. The absorbance was recorded by a Thermo Fisher Scientific microplate reader at 450 nm.

Dual-luciferase reporter assay. The potential interaction between circ_0001860 and miR-618 was prospected based on the complementary base pairing by the CircInteractome database platform (https://circinteractome.nia.nih.gov/), while potential interaction between miR-618 and HMGA2 was forecasted according to the TargetScan database platform (https://www.targetscan.org/vert_80/). To create luciferase reporter plasmids, circ_0001860 or HMGA2 wild-type (WT) and mutant (MUT) were inserted into the pGL3-Basic luciferase vector (Promega, Madison, WI, USA). Then, these WT or MUT plasmids were co-transfected into AGS or HGC-27 cells with miR-NC or miR-618 mimic using Lipofectamine 3000. After cells were transfected for 48 h, the luciferase activity was detected using a Dual-Luciferase Reporter Gene Assay Kit (RG027, Beyotime) following the operating handbook.

RNA immunoprecipitation (RIP) assays. The detection was executed by the Magna RIP™ RNA-Binding Protein Immunoprecipitation Kit (17-700, Millipore, Bedford, MA, USA) in line with the operation instructions. In brief, AGS or HGC-27 cell lines were lysed with RIP lysis buffer and then hatched with magnetic beads binding with anti-Ago2 or control IgG antibody (12-370, Millipore). Subsequently, the level of RNAs was determined by RT-qPCR.

RNA pull-down. The potential miRNAs of circ_0001860 were projected through the CircInteractome database platform (https://circinteractome.nia.nih.gov/). The Pierce Magnetic RNA-Protein Pull-Down Kit (Thermo Fisher) was used to perform the assay following the operating manual. Briefly, the biotinylated labeled circ_0001860 probes were treated with magnetic beads for 2 h at room temperature, and then the mixtures were further incubated with AGS cells overnight at 4 °C. After the magnetic beads were eluted, the captured miRNAs were determined using qRT-qPCR. Besides, the biotinylated labeled miR-618 probes were managed with magnetic beads for 2 h at room temperature, and then the mixtures were further hatched with AGS or HGC-27 cells overnight at 4 °C. After the magnetic beads were eluted, the captured circ_0001860 and HMGA2 were determined using qRT-qPCR. In addition, the biotinylated ZCCHC7 DNA probe was coated with beads via dissolution of the probe and cultured with Dynabeads M-280 Streptavidin (11205D, Invitrogen) for 10 min at room temperature. Then, cell lysates were cultured with the probe-coated beads. Eventually, the proteins were eluted and analyzed by using a western blot. The biotinylated probes were synthesized by Guangzhou Rinobio Co., Ltd (Guangdong, China)

Western blotting. To obtain the total proteins, AGS and HGC-27 cells were lysed using RIPA lysis buffer (R0010, Solarbio). The protein concentrations were measured with a BCA Protein Assay Kit (PC0020, Solarbio). After electrophoresing protein samples (20 μg) using 10% SDS-PAGE, the samples were transferred onto PVDF membranes (IPVH00010, Millipore). After being blocked with 5% BSA Blocking Buffer (SW3015, Solarbio) for 1 h at room temperature, the membranes were incubated with primary antibody against HMGA2 (1:5000, ab97276, Abcam, Cambridge, UK), EIF4A3 (1:1000, ab32485, Abcam), and β-actin (1:5000, ab8227, Abcam) at 4 °C overnight. The secondary antibody goat anti-rabbit IgG H&L (HRP) (1:10000, ab6721, Abcam) was then used to incubate the membranes for one hour at room temperature. The bands were developed by a BeyoECL Plus kit (P0018S, Beyotime), and the gray value was determined using Image-ProPlus software (Media Cybernetics, Inc., Rockville, MD, USA). Besides, to detect the nuclear and cytoplasmic expression of EIF4A3, AGS cells transfected with sh-NC and sh-circ_0001860 were treated with Nuclear and Cytoplasmic Protein Extraction Kit (P0028, Beyotime) according to the operating manual. LaminB (1:500, ab16048, Abcam) and H3 (1:5000, ab1791, Abcam) acted as the cytoplasmic and nuclear controls, respectively.

Animal experiments. Four-week-old BALB/c nude mice were supplied from HFK Bioscience (Beijing, China) and housed in pathogen-free conditions with a 12 h light-dark cycle and regulated temperature. Mice were randomly divided into the sh-NC group and the sh-circ_0001860 group

(n=5). In the sh-circ_0001860 group, 4×10^6 AGS cells with lentivirus-packaged sh-circ_0001860 described previously [16] were subcutaneously injected into the right flank of nude mice, whereas the animals in the sh-NC group received subcutaneously the same quantity of AGS cells with lentivirus-packaged sh-NC. Tumor volume was monitored for 7 days for consecutive 4 weeks and quantified by the following formula: volume = 0.5 × length × width^2. After five weeks, mice were sacrificed by breathing in too much isoflurane (#R510-22, RWD, Guangdong, China). The tumor samples were prepared for the immunohistochemistry tests by being ablated, weighed, and stored. All animal studies complied with the Guide for the Care and Use of Laboratory Animals and authorized by the Animal Research Ethics Committee of Harbin Medical University Cancer Hospital (approval number: YD2022-06).

Immunohistochemistry. The tumor tissues were dehydrated using gradient ethanol after being fixed in 4% paraformaldehyde. Then, tissues were immersed into paraffin (A601892, Sangon Biotech, Shanghai, China) and sectioned into 5 μm slices. The restoration was executed with sodium citrate solution (pH 6.0, E673002, Sangon Biotech) for 15 min at 94 °C. Subsequently, slices were blocked with 1% bovine serum albumin (BSA, A602449, Sangon Biotech) for 1 h and incubated with primary antibodies against HMGA2 (1:500, ab97276, Abcam), IFN-γ (1:100, PA5-95560, Invitrogen), and IL-10 (1:100, ab189392, Abcam) overnight at 4 °C. The secondary antibody HRP-labeled anti-rabbit IgG antibody (ab288151, Abcam) or HRP-marked anti-rat IgG antibody (ab6734, Abcam) was used to incubate with slices at 37 °C for 30 min. The slices were examined using an Olympus light microscope after re-staining with hematoxylin (G1080, Solarbio).

Table 1. Correlation between circ_0001860 expression and the clinical pathological features of 62 gastric cancer patients.

Characteristic	Cases	circ_0001860 level		p-value
		Low (n=31)	High (n=31)	
Age (years)				0.607
<60	26	14	12	
≥60	36	17	19	
Gender				0.200
Female	27	16	11	
Male	35	15	20	
Tumor size (cm)				0.070
<5	25	16	9	
≥5	37	15	22	
Lymph node metastasis				0.022*
Yes	29	10	19	
No	33	21	12	
TNM stage				0.010*
I+II	26	18	8	
III+IV	36	13	23	
Differentiation				0.610
Well and Moderate	28	15	13	
Poor	34	16	18	

Note: A chi-square test was utilized for comparing groups between low and high circ_0001860 expression. *p<0.05

Statistical analysis. The data were analyzed using IBM's SPSS 20.0 software and reported as mean ± standard deviation (SD) (Armonk, NY, USA). When identifying statistical differences between two or more groups, the Student's t-test or one-way analysis of variance (ANOVA) was used, followed by the *Post Hoc* Bonferroni test. The Kaplan-Meier plot produced the overall survival (OS), and the log-rank test was used to measure the difference. The chi-square test was used to examine the relationship between circ_0001860 level and clinical pathological characteristics. p<0.05 was defined as a significant difference.

Results

circ_0001860 was substantially expressed in gastric cancer. To uncover the function of circ_0001860 in gastric cancer, the circ_0001860 level was first detected in both tissues and cells of gastric cancer. The circ_0001860 level was increased in the gastric cancer tissues relative to that in adjacent control tissues (p<0.001, Figure 1A). Patients with gastric cancer who highly expressed circ_0001860 had a shorter OS (p=0.031, Figure 1B), more lymph node metastasis (p=0.022, Table 1), higher TNM stage (p=0.010, Table 1) than those with a low expression of circ_0001860. However, no statistically significant difference was detected between gastric cancer patients with high expression of circ_0001860 and low expression of circ_0001860 in terms of age (p=0.607), gender (p=0.200), tumor size (p=0.070), or differentiation (p=0.610) (Table 1). Additionally, an increased level of circ_0001860 was also found in HGC-27 and AGS cells (p<0.01, Figure 1C). Together, circ_0001860 was upregulated in gastric cancer, which indicated a dismal prognosis.

The inhibition of circ_0001860 resulted in a reduction in the growth, invasion, and immune escape of gastric cancer cells. To probe the action of circ_0001860 in the progression of gastric cancer, three shRNAs against circ_0001860 (sh-circ_0001860#1, 2, and 3) were used to downregulate the circ_0001860 expression in both HGC-27 and AGS cells. All three sh-circ_0001860 decreased the circ_0001860 level in both cell lines relative to sh-NC (p<0.05, Figure 2A), among which the interfering efficiency of sh-circ_0001860#2 was better than that of sh-circ_0001860#1 and 3. Thus, sh-circ_0001860#2 was chosen for the subsequent studies and designated as sh-circ_0001860. No statistical difference was discovered in the circ_0001860 level between the sh-NC group and the control group (p>0.05, Figure 2A). Transfection of sh-circ_0001860 declined the cell viability, the percent of EdU-positive cells and invaded cell numbers of both HGC-27 and AGS cells (p<0.01, Figures 2B–2E). Additionally, interference of circ_0001860 enhanced the concentra-

tions of IFN-γ and IL-2 but reduced the concentrations of IL-10 and TGF-β in the co-cultivation of PBMCs with tumor cell lines ($p<0.01$, Figures 2F, 2G). Taken together, the silencing of circ_0001860 repressed the growth, invasion, and immune evasion of gastric cancer cells.

circ_0001860 positively regulated the protein expression of HMGA2 by targeting miR-618. Given that circRNAs generally serve as ceRNAs to modulate gene expression by functioning on the molecular sponges of miRNA, the potential miRNAs were predicted by the CircInteractome online platform. There were 20 miRNAs predicted as the potential miRNAs of circ_0001860 (Figure 3A). Moreover, the biotinylated circ_0001860 probes enriched the most miR-618 based on the pull-down results ($p<0.001$, Figure 3A). Thus, miR-618 was chosen for further verification. To confirm the co-actions between circ_0001860 and miR-618, the miR-618 level was upregulated in HGC-27 and AGS cells by transfecting miR-618 mimics ($p<0.001$, Figure 3B) for the dual-luciferase reporter assay. The complementary base pairings between circ_0001860 and miR-618 and the schematic diagram of the construction of the dual-luciferase reporters are exhibited in Figure 3B. Co-transfection of miR-618 mimics and circ_0001860-WT, not circ_0001860-MUT, decreased the relative luciferase activity in the two cells ($p<0.01$, Figures 3C, 3D), indicating a direct bind between circ_0001860 and miR-618. Moreover, complementary base pairings were also found between miR-618 and HMGA2 (Figure 3E). Consistently, dual-luciferase reporter assays have proven the direct bind between miR-618 and HMGA2 ($p<0.01$, Figures 3F, 3G). RIP results revealed that the Ago2 group enriched more circ_0001860 and miR-618 relative to the IgG group ($p<0.001$, Figure 3H), and RNA pull-down results exhibited that the biotinylated miR-618 probes enriched for circ_0001860 and HMGA2 relative to the NC probes ($p<0.001$, Figures 3I, 3J) in both cell lines. The miR-618 level was decreased with the administration of anti-miR-618 ($p<0.01$, Figure 3K). Silencing of circ_0001860 diminished the HMGA2 expression in the two cells, which was rescued with the treatment of anti-miR-618 ($p<0.01$, Figure 3L). Altogether, circ_0001860 positively modulated the protein expression of HMGA2 by targeting miR-618.

circ_0001860 promoted the growth, invasion, and immune evasion of gastric cancer cells by the miR-618/HMGA2 pathway. To verify the role of circ_0001860 in the malignant progressions of gastric cancer through the miR-618/HMGA2 axis, the HMGA2 expression was upregulated in AGS cells ($p<0.01$, Figure 4A). Transfection of sh-circ_0001860 into AGS cells reduced the cell viability and invaded cell numbers ($p<0.01$), which were recovered with the knockdown of miR-618 ($p<0.05$) or overexpression of HMGA2 ($p<0.01$, Figures 4B–4D). Additionally, knockdown of miR-618 or overexpression of HMGA2 counteracted the IFN-γ concentration but restored the IL-10 concentration in AGS cells transfected with sh-circ_0001860 ($p<0.05$, Figures 4E, 4F). Overall, circ_0001860 enhanced the growth, invasion, and immune evasion of gastric cancer cells through the miR-618/HMGA2 axis.

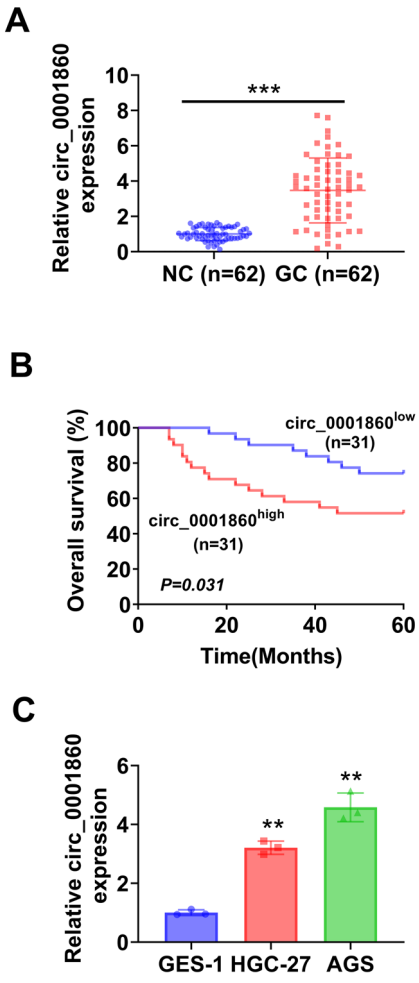

Figure 1. Upregulation of circ_0001860 indicated a poor prognosis in the gastric cancer patients. A) The expression level of circ_0001860 was detected by RT-qPCR in a pair of 62 gastric cancer tissues and adjacent normal control tissues from gastric cancer patients. Data were expressed after being normalized with *GAPDH*. ***$p<0.001$. B) Sixty-two gastric cancer patients were divided into the low circ_0001860 expression group (n=31) and the high circ_0001860 expression group (n=31) based on the median circ_0001860 expression value in Figure 1A as the cut-off value. OS of these two groups was evaluated by the Kaplan–Meier survival curve. C) The expression level of circ_0001860 was examined by RT-qPCR in gastric cancer cell lines, HGC-27, and AGS cells. Data were expressed after being normalized with *GAPDH*. **$p<0.01$ vs. GSE-1.

The RNA-binding protein EIF4A3 modulated the expression of circ_0001860. Besides, the upstream gene regulation of circ_0001860 was probed. Based on the CircInteractome online results, EIF4A3 owned four binding sites on the upstream region of circ_0001860, including a binding site on the mRNA of the circ_0001860 ring-forming gene ZCCHC7 (Figure 5A). Pull-down results displayed that there was an enrichment between the EIF4A3 protein and ZCCHC7

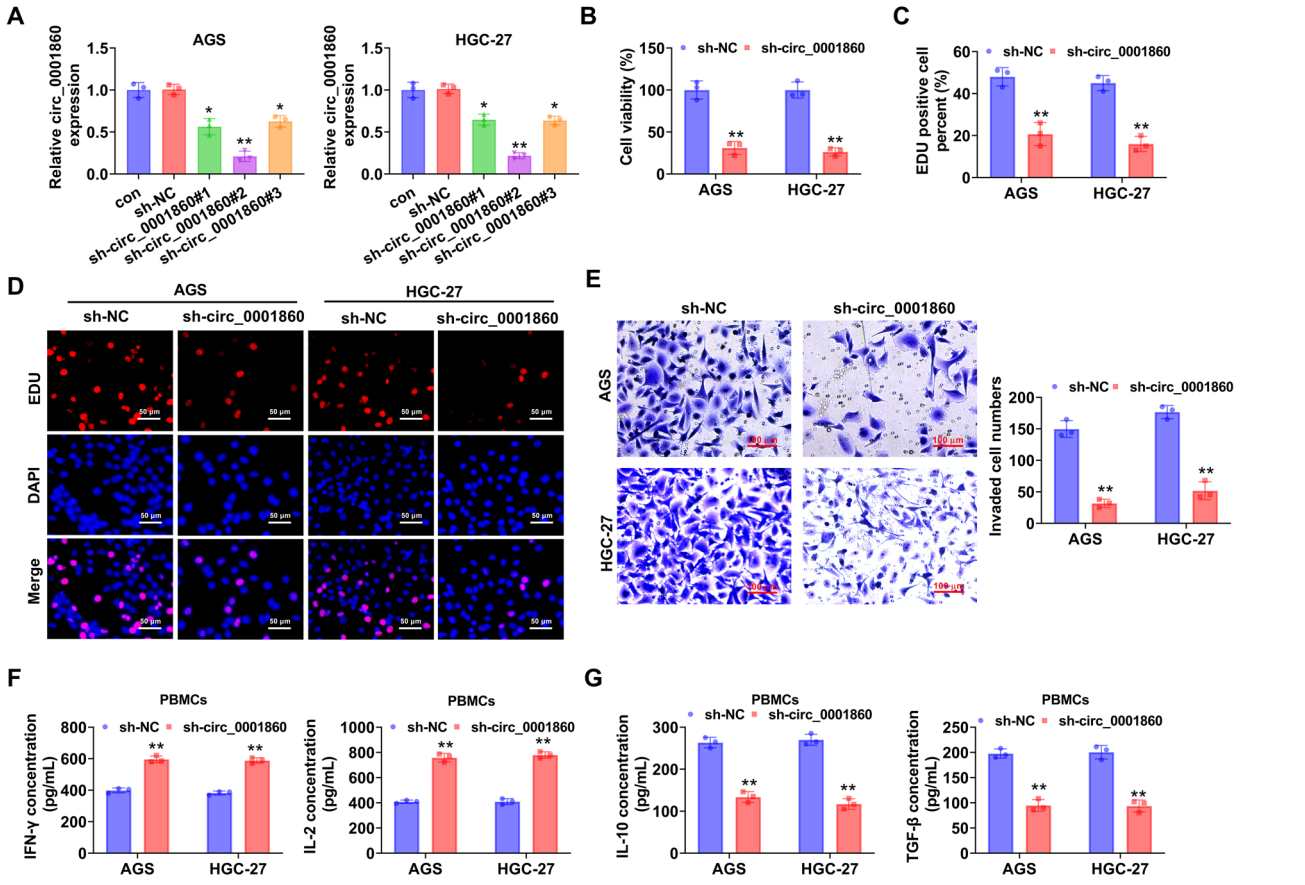

Figure 2. Interference of circ_0001860 suppressed the proliferation, invasion, and immune escape of gastric cancer cells. A) The interfering efficiency of three sh-circ_0001860 was detected by RT-qPCR. Data were expressed after being normalized with *GAPDH*. B) Examination of HGC-27 and AGS cell viability by CCK-8 assays. C, D) The proliferation ability of HGC-27 and AGS cells was assessed by EdU staining. Scale bar = 50 μm. E) The invasion ability was determined by Transwell assays. Scale bar = 100 μm. F) Measurement of the concentrations of IFN-γ and IL-2 by ELISA. G) Detection of the concentrations of IL-10 and TGF-β by ELISA. *p<0.05 and **p<0.01 vs. sh-NC.

mRNA rather than control (Figure 5B). Moreover, RIP results by using the EIF4A3 antibody showed that fragments a and b were enriched in EIF4A3 precipitates after the RT-qPCR examination with the primers based on the four predicted binding regions (p<0.001, Figure 5C). The EIF4A3 expression was diminished or fostered in AGS cells by transfecting sh-EIF4A3 or EIF4A3 overexpression plasmid, respectively (p<0.01, Figure 5D). Knockdown of EIF4A3 decreased the circ_0001860 expression, while overexpression of EIF4A3 increased the circ_0001860 level in AGS cells (p<0.01, Figure 5E). Besides, silencing circ_0001860 has no influence on the nuclear and cytoplasmic expression of eIF4A3 (p>0.05, Figure 5F). Collectively, EIF4A3 positively modulated the circ_0001860 expression in gastric cancer cells.

Knockdown circ_0001860 suppressed proliferation and immune escape of gastric cancer *in vivo*. Furthermore, the role of circ_0001860 was surveyed in mice with lentivirus-packaged sh-circ_0001860. Mice with sh-circ_0001860 exhibited a smaller tumor size and lighter weight than mice with sh-NC (p<0.01), while there was no discernible statistical difference in the mice's body weight between the two groups (Figures 6A–6C). Knockdown of circ_0001860 elevated the expression level of miR-618 and the IFN-γ level while declining the level of HMGA2 and IL-10 in tumor tissues (p<0.01, Figures 6D, 6E). Together, silencing of circ_0001860 repressed gastric cancer cell growth and immune escape involved in the miR-618/HMGA2 axis in xenografted mice.

Discussion

Gastric cancer is a type of digestive system malignancy with a high invasion that is one of the most common and deadly cancers in the world [17]. Gastric cancer is characterized by vague early symptoms, which brings great resistance to diagnosis and treatment. Thus, screening potential targets is necessary and important for the detection and treatment of gastric cancer. This study found that circ_0001860 was upregulated in gastric cancer, indicating a dismal prognosis

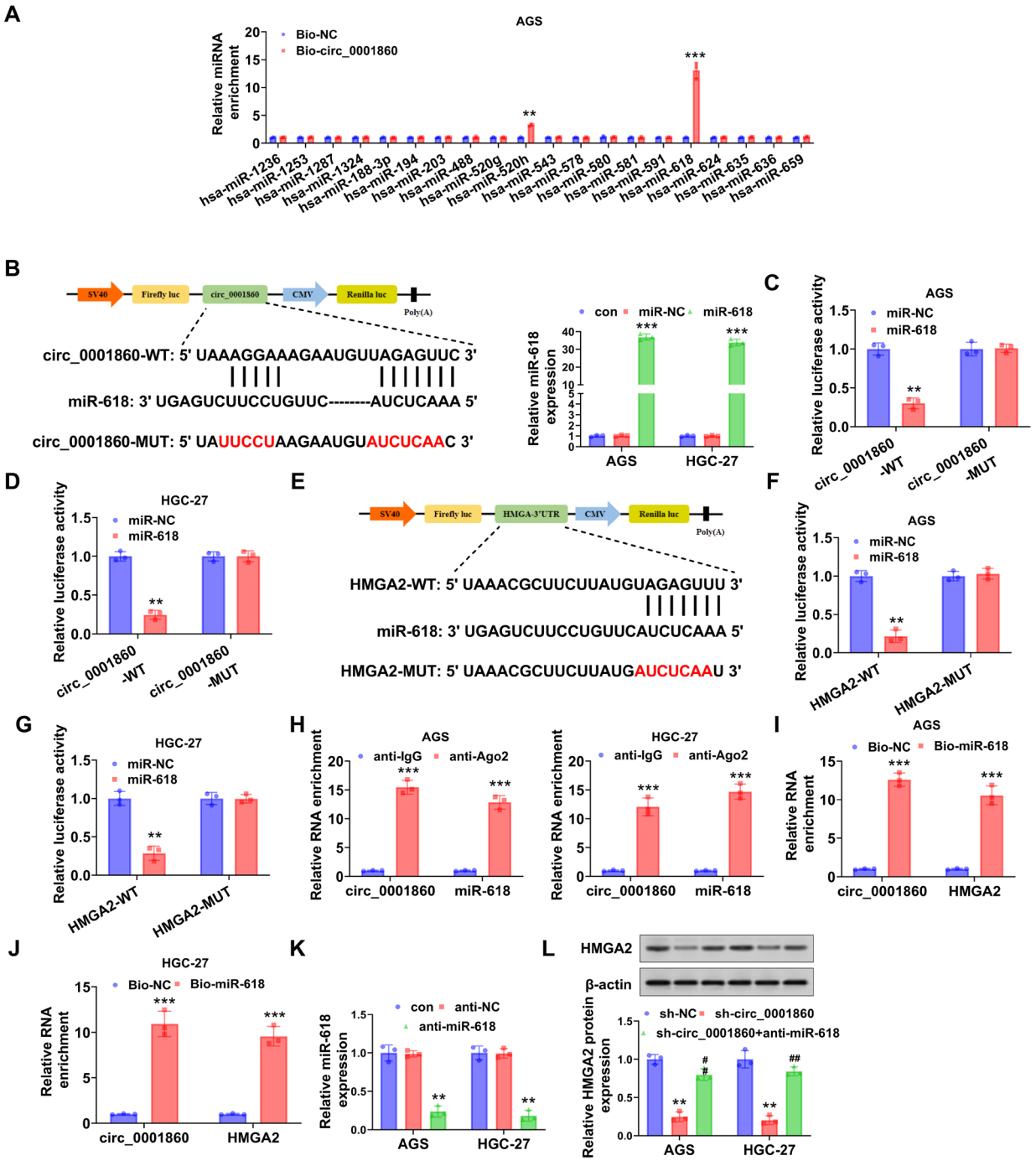

Figure 3. circ_0001860 positively regulated the protein expression of HMGA2 by targeting miR-618. A) The binding sites between circ_0001860 and miR-618 were predicted by the CircInteractome online platform, and the wild-type and mutant sequences of circ_0001860 were also designed and exhibited. B) The overexpression efficiency of miR-618 was detected by qRT-PCR. The data were normalized with *U6*. ***p<0.001 vs. miR-NC. C) The luciferase activities were determined in AGS cells by the Dual-Luciferase Reporter Assay System. **p<0.01 vs. miR-NC. D) The luciferase activities were determined in HGC-27 cells by the Dual-Luciferase Reporter Assay System. **p<0.01 vs. miR-NC. E) The binding sites between miR-618 and HMGA2 were predicted by the Targetscan online platform, and the wild-type and mutant sequences of HMGA2 were also designed and exhibited. F) The luciferase activities were determined in AGS cells by the Dual-Luciferase Reporter Assay System. **p<0.01 vs. miR-NC. G) The luciferase activities were determined in HGC-27 cells by the Dual-Luciferase Reporter Assay System. **p<0.01 vs. miR-NC. H) RIP results showed that the Ago2 group enriched more circ_0001860 and miR-618 compared. ***p<0.001 vs. anti-IgG. I, J) RNA pull-down results exhibited that the biotinylated miR-618 probes enriched for circ_0001860 and HMGA2. ***p<0.001 vs. Bio-NC. K) The knockdown efficiency of miR-618 was detected by qRT-PCR. The data were normalized with *U6*. **p<0.01 vs. anti-NC. L) The relative protein expression of HMGA2 was detected by western blot. Data were normalized with β-actin. **p<0.01 vs. sh-NC; ##p<0.01 vs. sh-circ_0001860

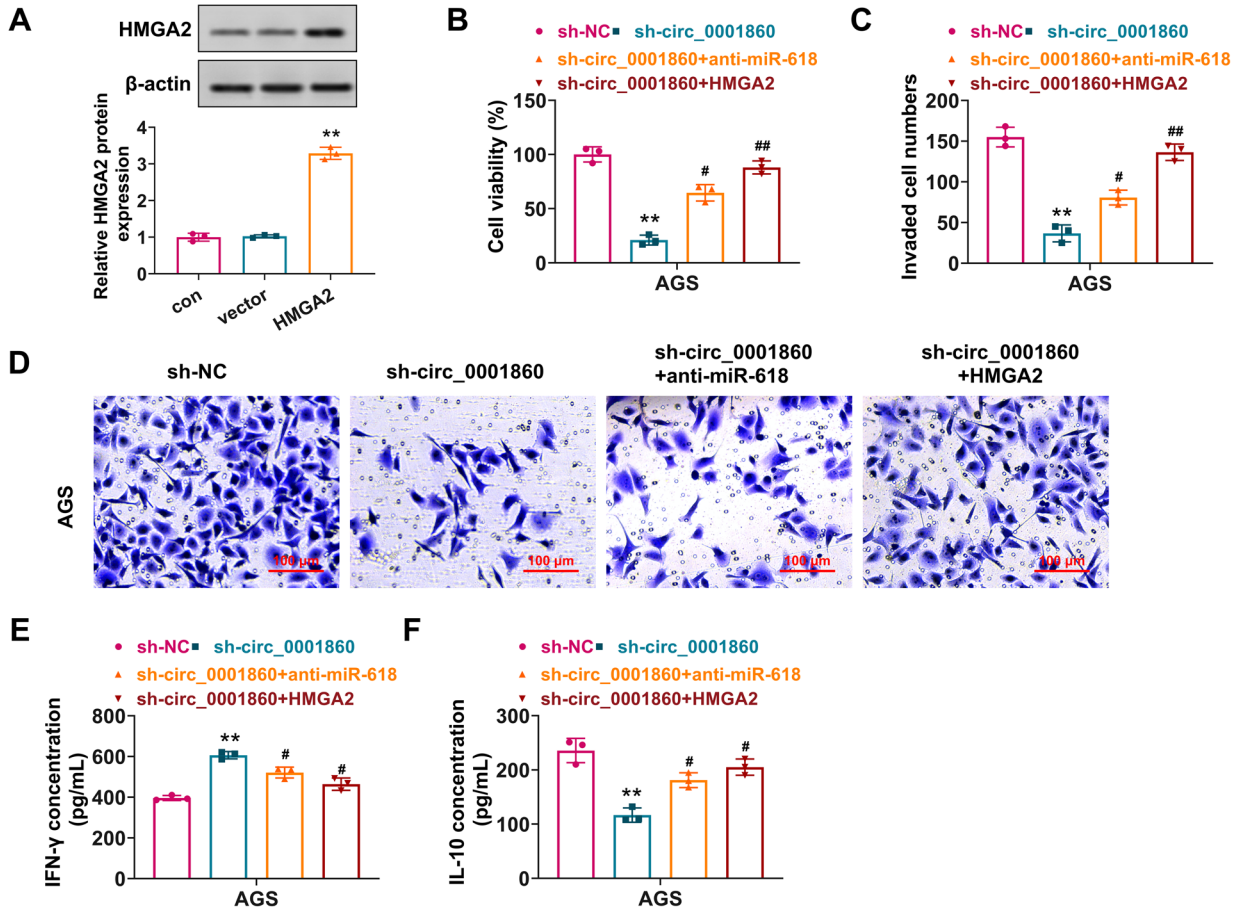

Figure 4. circ_0001860 facilitated the proliferation, invasion, and immune escape of gastric cancer cells via the miR-618/HMGA2 pathway. A) The overexpression efficiency of HMGA2 was detected by a western blot. The data were normalized with β-actin. **p<0.01 vs. vector. B) Examination of cell viability by CCK-8 assays. **p<0.01 vs. sh-NC; #p<0.05 and ##p<0.01 vs. sh-circ_0001860. C, D) Determination of cell invasion ability by Transwell assays. Scale bar = 100 μm. **p<0.01 vs. sh-NC; #p<0.05 and ##p<0.01 vs. sh-circ_0001860. E) Measurement of the IFN-γ concentration by ELISA. **p<0.01 vs. sh-NC; #p<0.05 vs. sh-circ_0001860. F) Detection of the IL-10 concentration by ELISA. **p<0.01 vs. sh-NC; #p<0.05 vs. sh-circ_0001860

for gastric cancer patients. Knockdown of circ_0001860 suppressed growth, invasion, and immune evasion of gastric cancer cells. circ_0001860 sponged miR-618 to positively modulate the HMGA2 level in gastric cancer cells. The inhibitory role of sh-circ_0001860 on growth, invasion, and immune evasion of gastric cancer cells was abolished with the miR-618 knockdown or the HMGA2 overexpression. Besides, EIF4A3 positively modulated the circ_0001860 level in gastric cancer cells. *In vivo*, silencing of circ_0001860 reduced tumor size and weight, the expression of HMGA2 and IL-10, and enhanced the level of miR-618 and IFN-γ. Taken together, EIF4A3 protein regulated the expression of circ_0001860 by binding to the mRNA of the circ_0001860 ring-forming gene ZCCHC7, and then circ_0001860 enhanced growth, invasion, and immune evasion of gastric cancer cells through the miR-618/HMGA2 axis (Figure 7).

The levels of different circRNAs have been demonstrated to be dysregulated in gastric cancer, which indicates that circRNAs can serve as the target for the detection and management of gastric cancer [18]. circ_0001860, the research target of the current study, has been revealed to be lowly expressed in medroxyprogesterone acetate-resistant endometrial cancer cell lines and tissues and negatively related to histological grade and lymph node metastasis of patients with endometrial cancer [15]. Here, we discovered that circ_0001860 was upregulated in gastric cancer tissues and cell lines and indicated shorter OS, more lymph node metastasis, and higher TNM stage in gastric cancer patients. Thus, these findings suggested that upregulation of circ_0001860 in gastric cancer forecasted the dismal prognosis of gastric cancer patients.

Dysregulation of circ_0001860 in gastric cancer indicated that it might play a role in the development of gastric cancer. Here, we discovered that the knockdown of circ_0001860 reduced gastric cancer cell viability, the percent of EdU-positive cells, the invaded cell numbers,

and the concentrations of IL-10 and TGF-β but fostered the concentrations of IFN-γ and IL-2. Additionally, the knockdown of circ_0001860 inhibited tumor size and weight and the IL-10 level but enhanced the IFN-γ level in xenografted mice. These results revealed that silencing of circ_0001860 suppressed growth, invasion, and immune escape of gastric cancer cells. The ability to proliferate and then invade is the basic and remarkable characteristic of all types of cancers, including gastric cancer [19]. CircRNAs have been demonstrated to mediate all aspects of gastric cancer, including proliferation, invasion, apoptosis, mobility, and drug resistance [20]. Besides, immune escape has been identified as one of the significant hallmarks of cancers [19]. An important carcinogenesis regulator that governs the course of tumor

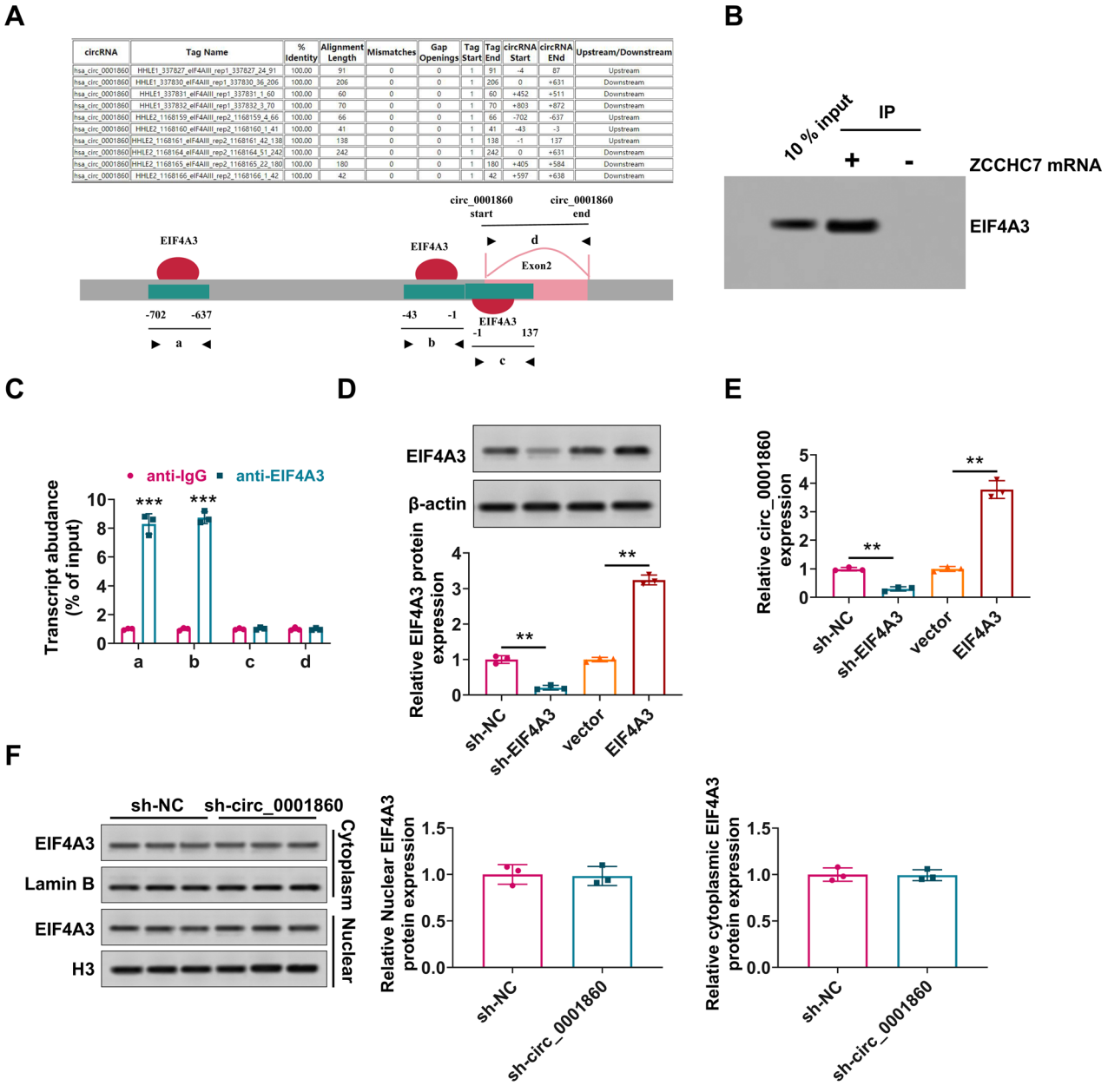

Figure 5. EIF4A3 positively modulated the circ_0001860 level in gastric cancer cells. A) The binding sites for EIF4A3 on the upstream region of circ_0001860 were predicted from CircInteractome. B) Pull-down assay demonstrated the enrichment of EIF4A3 protein in ZCCHC7 mRNA pull-down. C) RT-qPCR following the EIF4A3-RIP assay confirmed the binding of EIF4A3 on the predicted binding region (a, b, c, and d) of circ_0001860. ***p<0.001 vs. anti-IgG. D) The relative protein expression of EIF4A3 was detected in AGS cells by a western blot. Data were normalized with β-actin. **p<0.01. E) The expression level of circ_0001860 was examined by RT-qPCR in AGS cells. Data were expressed after being normalized with *GAPDH*. **p<0.01

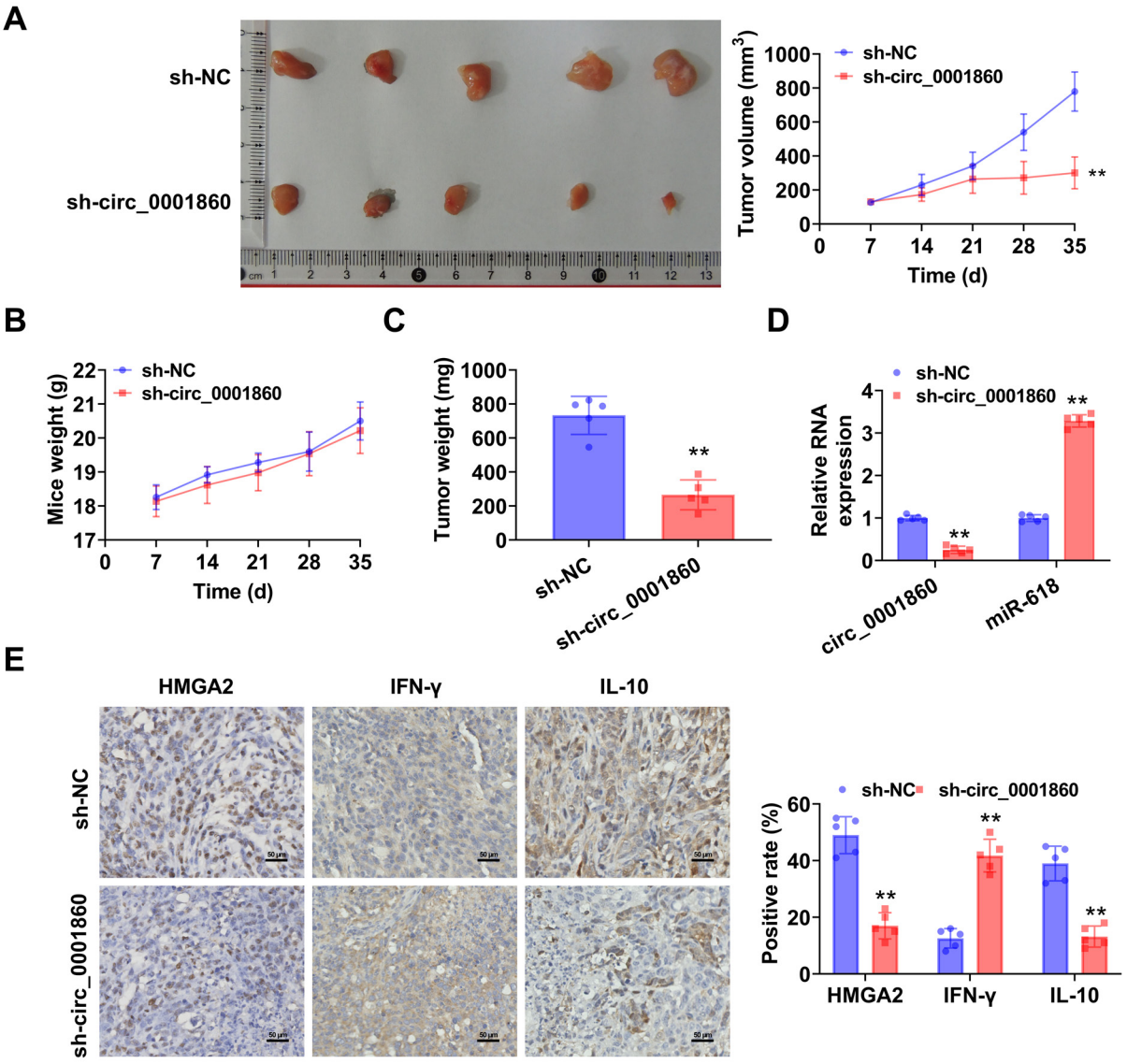

Figure 6. Knockdown of circ_0001860 inhibited gastric cancer cell growth and immune escape involved in the miR-618/HMGA2 axis in xenografted mice. Nude mice were subcutaneously inoculated with a total of 4×10^6 AGS cells with lentivirus-packaged sh-circ_0001860 into the right flank of nude mice. A) Representative images of neoplasms from nude mice (left) and monitoring of tumor volume every one week for four successive weeks (right). Tumor volume was quantified by the following formula: volume = 0.5 × length × width². B) Supervision of mice body weight every one week for four successive weeks. C) Measurement of tumor weight after five weeks. D) The expression level of circ_0001860 and miR-618 was examined by RT-qPCR in tumor tissues. Data were expressed after being normalized with *GAPDH* or *U6*. **p<0.01. E) The expression levels of HMGA2, IFN-γ, and IL-10 in tumor tissues were detected by immunohistochemistry. Scale bar = 50 μm. **p<0.01 vs. sh-NC.

formation and progression as well as the tumor response to immunotherapy is the immunological composition of the tumor microenvironment, which is made up of a variety of tumor cells, immune cells, stromal cells, and immune cytokines [21]. The principal mechanism for tumor cell clearance inside the tumor immunological microenvironment is the adaptive cellular immune response, which is primarily driven by effector T cells, including CD4+ and CD8+ T cells. Apart from maturing into CD4+ helper T cells, activated CD4+ T cells can also release IL-2 to enable CD8+ cytotoxic lymphocytes, which are prerequisites for the elimination of tumor cells [22]. Besides, there are numerous types of CD4+ T cell responses for anti-tumor immunity, depending on the cytokine composition of the cells [23]. Th1 cells are mainly identified by their production of IFN-γ, whereas Th2, Th3, and Tr1 cells secrete TGF-β, IL-4, IL-5, and IL-10. Since Th1 primarily promotes cellular immunity while the others often boost humoral immunity, the balance of Th1/Th2/

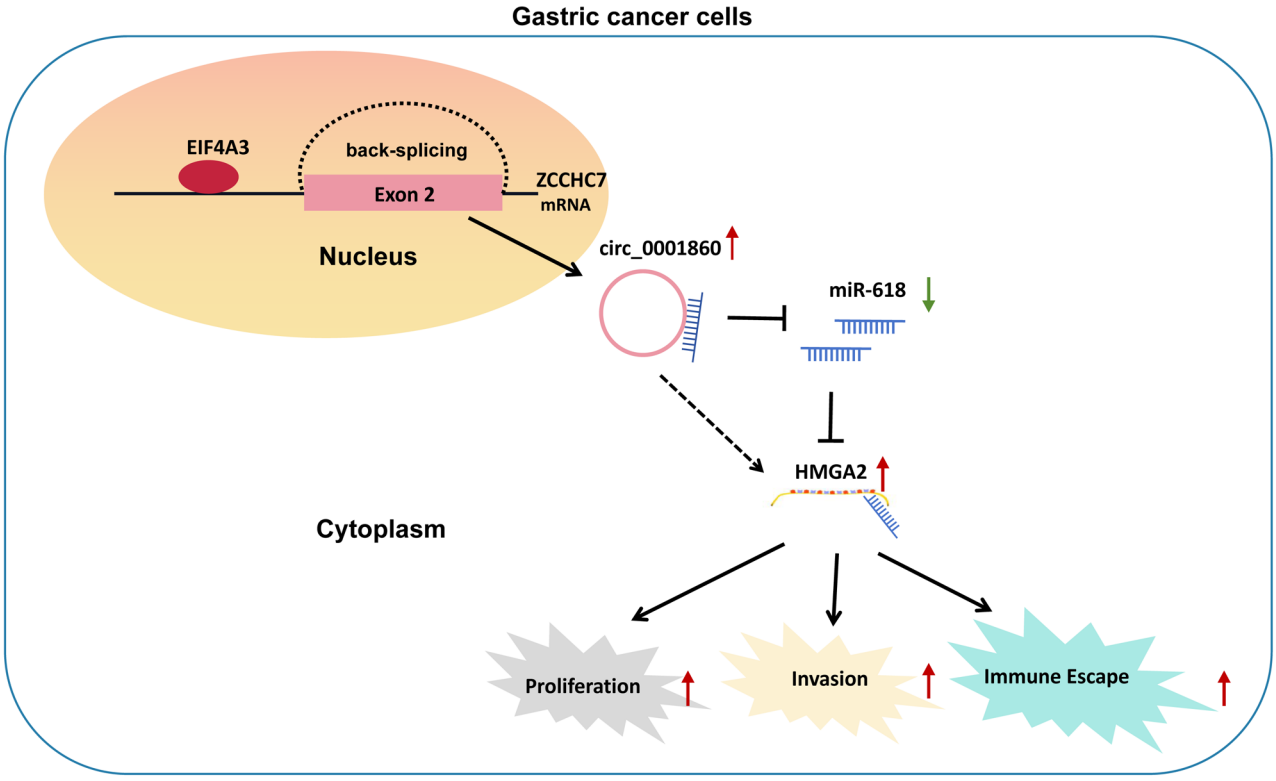

Figure 7. A schematic diagram describing that EIF4A3 protein regulated the expression of circ_0001860 by binding to the mRNA of the circ_0001860 ring-forming gene ZCCHC7. circ_0001860 was upregulated in gastric cancer, and circ_0001860 enhanced proliferation, invasion, and immune escape of gastric cancer cells through the miR-618/HMGA2 axis.

Th3/Tr1 cytokines undoubtedly influences the outcome of distinct immune responses. In essence, a Th1/Th2/Th3/Tr1 cytokine profile promotes pro-tumor activity, while a Th1 cytokine profile facilitates an anti-tumor response. The Th1-/Th2-shift is a critical indicator of inadequate cellular defense during carcinogenesis, characterized by a change in profile from a Th1 to a Th2/Th3/Tr1 one [24]. Different circRNAs have been reported to function on immune escape in gastric cancer, such as circ_0136666 [25], circ_0001479 [26], circS-CUBE3 [27], circ_0008287 [28], and circDLG1 [29]. Besides, the knockdown of circ_0001860 was shown to accelerate growth and suppress apoptosis and medroxyprogesterone acetate sensitivity in endometrial cancer [15]. Taken together, the downregulation of circ_0001860 repressed proliferation, invasion, and immune escape of gastric cancer cells.

The most prominent characteristic of circRNAs is that they serve as the molecular sponges of miRNA through the ceRNA mechanism to modulate gene expressions [30]. Miao et al. [25] reported that circ_0136666 sponged miR-375 to regulate the PRKDC expression, thereby promoting proliferation and immune escape of gastric cancer. circ_0008287 augmented proliferation, migration, and invasion of gastric cancer cells by gastric cancer through miR-548c-3p/CLIC1 [28]. Similar outcomes were shown in circDLG1 by the miR-141-3p/CXCL12 axis [29]. In the current study, the luciferase reporter, RIP, and pull-down assays verified the direct association between miR-618 and circ_0001860, which was predicted to be the target. miR-618 was reported to be downregulated in gastric cancer tissues, and miR-618 repressed cell mobility and invasion of gastric cancer [31]. Besides, miR-618 was also proven to be sponged by circRNACCDC66 to regulate the BCL2 expression, thereby mediating cisplatin resistance in gastric cancer [32]. Further analysis showed that miR-618 could directly bind with HMGA2 in this study. HMGA2 is immensely expressed in gastric cancer and is significantly correlated with the dismal clinical prognosis of gastric cancer patients [33]. HMGA2 is also strongly relevant to the immune infiltration and immune escape of gastric cancer [33]. Moreover, HMGA2 takes part in various progresses of gastric cancer, including epithelial-mesenchymal transitions [34], stemness [34, 35], motility [35, 36], vasculogenic mimicry [36], and invasion [36]. Furthermore, HMGA2 can be directly bound by different miRNAs to mediate the progression and development of gastric cancer, such as miR-128 [37], miR-491 [38], and miR-503 [39]. More importantly, Cai et al. [40] reported that circ_0000267 by miR-503-5p/HMGA2 axis contributed to proliferation, metastasis, and epithelial-mesenchymal transitions of gastric

cancer. Xia et al. [41] revealed that circFAM73A enhanced the cancer stem cell-like characteristics via the miR-490-3p/HMGA2 axis in gastric cancer. In addition, our outcomes discovered that the knockdown of circ_0001860 reduced the HMGA2 expression in gastric cancer cells, which was rescued with the treatment of anti-miR-618. Altogether, these findings indicated that circ_0001860 positively modulated the protein expression of HMGA2 by targeting miR-618.

Except for the mechanisms that circRNAs function as miRNA sponges, circRNAs can bind to RNA-binding proteins to modulate the expression of target genes and eventually control the growth and metastasis of gastric cancer [18]. EIF4A3, a crucial modulator of RNA splicing [42], binds to the upstream region of MMP9 mRNA and promotes the formation of circular RNA to evoke circ-MMP9 expression [43]. In gastric cancer, EIF4A3 binds and induces a variety of circRNAs to participate in different progresses. For instance, EIF4A3 bound circ_0006847 to enhance apoptosis and G0/G1 arrest and inhibited proliferation, migration, and invasion in gastric cancer [44]. EIF4A3 binds and modulates the expression of circGLIS3 [13], circABCA5 [45], circ_0074027 [46], circ_100290 [47], and circ_001988 [48] to facilitate growth, mobility, and invasion of gastric cancer cells. Here, EIF4A3 was identified to have binding sites on the upstream region of circ_0001860, which was proven by RIP and pull-down assays. Moreover, the knockdown of EIF4A3 decreased the circ_0001860 expression, while overexpression of EIF4A3 increased the circ_0001860 level in AGS cells. Besides, there was no influence of silencing circ_0001860 on the nuclear and cytoplasmic expression of EIF4A3, indicating that the nuclear import of EIF4A3, the upstream regulator of circ_0001860, was not affected by circ_0001860. The study from Jiang et al. [49] identified EIF4A3 as the downstream of circ467, and the nuclear import of EIF4A3 was affected by circ467. Thus, these results indicated the diversity between EIF4A3 and circRNAs regulation. Collectively, these outcomes suggested that EIF4A3 positively modulated the circ_0001860 expression in gastric cancer cells.

In summary, our data expounded that the circ_0001860 level was upregulated in gastric cancer, which indicated a dismal prognosis. Knockdown of circ_0001860 suppressed growth, invasion, and immune escape of gastric cancer cells. Mechanically, circ_0001860 sponged miR-618 to modulate the HMGA2 expression, thereby mediating the progression of gastric cancer. Besides, EIF4A3 positively modulated the expression of circ_0001860 in gastric cancer cells. Nevertheless, several limitations still need to be discussed in our following study. For instance, the role of circ_0001860 in other malignant progresses of gastric cancer, such as migration, apoptosis, epithelial-mesenchymal transitions, and stemness, may be explored in the subsequent study. Additionally, the direct effect of the circ_0001860/miR-618/HMGA2 axis should also be investigated in *in vivo* experiment. Briefly, our findings offer a potential target for the clinical detection and treatment of gastric cancer.

Supplementary information is available in the online version of the paper.

References

[1] SUNG H, FERLAY J, SIEGEL RL, LAVERSANNE M, SOERJOMATARAM I et al. Global Cancer Statistics 2020: GLOBOCAN Estimates of Incidence and Mortality Worldwide for 36 Cancers in 185 Countries. CA Cancer J Clin 2021; 71: 209–249. https://doi.org/10.3322/caac.21660

[2] HÖGNER A, MOEHLER M. Immunotherapy in Gastric Cancer. Curr Oncol 2022; 29: 1559–1574. https://doi.org/10.3390/curroncol29030131

[3] ENGSTRAND L, GRAHAM DY. Microbiome and Gastric Cancer. Dig Dis Sci 2020; 65: 865–873. https://doi.org/10.1007/s10620-020-06101-z

[4] BESSÈDE E, MÉGRAUD F. Microbiota and gastric cancer. Semin Cancer Biol 2022; 86: 11–17. https://doi.org/10.1016/j.semcancer.2022.05.001

[5] ZHAO Q, CAO L, GUAN L, BIE L, WANG S et al. Immunotherapy for gastric cancer: dilemmas and prospect. Brief Funct Genomics 2019; 18: 107–112. https://doi.org/10.1093/bfgp/ely019

[6] LI P, HUANG CM, ZHENG CH, RUSSO A, KASBEKAR P et al. Comparison of gastric cancer survival after R0 resection in the US and China. J Surg Oncol 2018; 118: 975–982. https://doi.org/10.1002/jso.25220

[7] CHEN W, ZHENG R, BAADE PD, ZHANG S, ZENG H et al. Cancer statistics in China, 2015. CA Cancer J Clin 2016; 66: 115–132. https://doi.org/10.3322/caac.21338

[8] LEI M, ZHENG G, NING Q, ZHENG J, DONG D. Translation and functional roles of circular RNAs in human cancer. Mol Cancer 2020; 19: 30. https://doi.org/10.1186/s12943-020-1135-7

[9] LIM TB, LAVENNIAH A, FOO RS. Circles in the heart and cardiovascular system. Cardiovasc Res 2020; 116: 269–278. https://doi.org/10.1093/cvr/cvz227

[10] FLORIS G, ZHANG L, FOLLESA P, SUN T. Regulatory Role of Circular RNAs and Neurological Disorders. Mol Neurobiol 2017; 54: 5156–5165. https://doi.org/10.1007/s12035-016-0055-4

[11] ZHOU Z, SUN B, HUANG S, ZHAO L. Roles of circular RNAs in immune regulation and autoimmune diseases. Cell Death Dis 2019; 10: 503. https://doi.org/10.1038/s41419-019-1744-5

[12] LIU A, LIANG J, WEN J. CircNRD1 elevates THAP domain containing 11 through sequestering microRNA-421 to inhibit gastric cancer growth and tumorigenesis. J Biochem Mol Toxicol 2024; 38: e23705. https://doi.org/10.1002/jbt.23705

[13] ZHANG Y, WANG X, LIU W, LEI T, QIAO T et al. CircGLIS3 promotes gastric cancer progression by regulating the miR-1343-3p/PGK1 pathway and inhibiting vimentin phosphorylation. J Transl Med 2024; 22: 251. https://doi.org/10.1186/s12967-023-04625-2

[14] FU M, GU J, YU D, WANG M, ZHANG J et al. Circ1811 suppresses gastric cancer progression by regulating the miR-632/DAPK1 axis. Gene 2024; 910: 148331. https://doi.org/10.1016/j.gene.2024.148331

[15] YUAN S, ZHENG P, SUN X, ZENG J, CAO W et al. Hsa_Circ_0001860 Promotes Smad7 to Enhance MPA Resistance in Endometrial Cancer via miR-520h. Front Cell Dev Biol 2021; 9: 738189. https://doi.org/10.3389/fcell.2021.738189

[16] DONG CR, HU DX, LIU SC, LUO HL, ZHANG WJ. AKT/GSK-3beta/VEGF signaling is involved in P2RY2 activation-induced the proliferation and metastasis of gastric cancer. Carcinogenesis 2023; 44: 65–79. https://doi.org/10.1093/carcin/bgac095

[17] SMYTH EC, NILSSON M, GRABSCH HI, VAN GRIEKEN NC, LORDICK F. Gastric cancer. Lancet 2020; 396: 635–648. https://doi.org/10.1016/s0140-6736(20)31288-5

[18] MA Q, YANG F, XIAO B, GUO X. Emerging roles of circular RNAs in tumorigenesis, progression, and treatment of gastric cancer. J Transl Med 2024; 22: 207. https://doi.org/10.1186/s12967-024-05001-4

[19] HANAHAN D. Hallmarks of Cancer: New Dimensions. Cancer Discov 2022; 12: 31–46. https://doi.org/10.1158/2159-8290.Cd-21-1059

[20] XIA K, WANG Z, LIU B, WANG W, LIU Y et al. Functions of circular RNAs and their potential applications in gastric cancer (Review). Oncol Lett 2023; 25: 217. https://doi.org/10.3892/ol.2023.13803

[21] OSTRAND-ROSENBERG S, SINHA P, BEURY DW, CLEMENTS VK. Cross-talk between myeloid-derived suppressor cells (MDSC), macrophages, and dendritic cells enhances tumor-induced immune suppression. Semin Cancer Biol 2012; 22: 275–281. https://doi.org/10.1016/j.semcancer.2012.01.011

[22] Shrihari TG. Innate and adaptive immune cells in Tumor microenvironment. Gulf J Oncolog 2021; 1: 77–81.

[23] MOSMANN TR, SAD S. The expanding universe of T-cell subsets: Th1, Th2 and more. Immunol Today 1996; 17: 138–146. https://doi.org/10.1016/0167-5699(96)80606-2

[24] ROMAGNANI S. The Th1/Th2 paradigm. Immunol Today 1997; 18: 263–266. https://doi.org/10.1016/s0167-5699(97)80019-9

[25] MIAO Z, LI J, WANG Y, SHI M, GU X et al. Hsa_circ_0136666 stimulates gastric cancer progression and tumor immune escape by regulating the miR-375/PRKDC Axis and PD-L1 phosphorylation. Mol Cancer 2023; 22: 205. https://doi.org/10.1186/s12943-023-01883-y

[26] ZANG J, XIAO L, SHI X, LIU S, WANG Y et al. Hsa_circ_0001479 accelerates tumorigenesis of gastric cancer and mediates immune escape. Int Immunopharmacol 2023; 124: 110887. https://doi.org/10.1016/j.intimp.2023.110887

[27] SHAN H, ZHANG X, ZHANG X, WEI Y, MENG L et al. CircSCUBE3 Reduces the Anti-gastric Cancer Activity of Anti-PD-L1. Mol Biotechnol 2024; 66: 123–137. https://doi.org/10.1007/s12033-023-00696-0

[28] LI B, LIANG L, CHEN Y, LIU J, WANG Z et al. Circ_0008287 promotes immune escape of gastric cancer cells through impairing microRNA-548c-3p-dependent inhibition of CLIC1. Int Immunopharmacol 2022; 111: 108918. https://doi.org/10.1016/j.intimp.2022.108918

[29] CHEN DL, SHENG H, ZHANG DS, JIN Y, ZHAO BT et al. The circular RNA circDLG1 promotes gastric cancer progression and anti-PD-1 resistance through the regulation of CXCL12 by sponging miR-141-3p. Mol Cancer 2021; 20: 166. https://doi.org/10.1186/s12943-021-01475-8

[30] PANDA AC. Circular RNAs Act as miRNA Sponges. Adv Exp Med Biol 2018; 1087: 67–79. https://doi.org/10.1007/978-981-13-1426-1_6

[31] SHI J, GONG L, CHEN L, LUO J, SONG G et al. miR-618 Suppresses Metastasis in Gastric Cancer by Downregulating the Expression of TGF-β2. Anat Rec (Hoboken) 2019; 302: 931–940. https://doi.org/10.1002/ar.24083

[32] ZHANG Q, MIAO Y, FU Q, HU H, CHEN H et al. CircRNACCDC66 regulates cisplatin resistance in gastric cancer via the miR-618/BCL2 axis. Biochem Biophys Res Commun 2020; 526: 713–720. https://doi.org/10.1016/j.bbrc.2020.03.156

[33] WU Z, HUANG Y, YUAN W, WU X, SHI H et al. Expression, tumor immune infiltration, and prognostic impact of HMGs in gastric cancer. Front Oncol 2022; 12: 1056917. https://doi.org/10.3389/fonc.2022.1056917

[34] LI W, WANG Z, ZHA L, KONG D, LIAO G et al. HMGA2 regulates epithelial-mesenchymal transition and the acquisition of tumor stem cell properties through TWIST1 in gastric cancer. Oncol Rep 2017; 37: 185–192. https://doi.org/10.3892/or.2016.5255

[35] SUN J, SUN B, ZHU D, ZHAO X, ZHANG Y et al. HMGA2 regulates CD44 expression to promote gastric cancer cell motility and sphere formation. Am J Cancer Res 2017; 7: 260–274.

[36] SUN J, SUN B, SUN R, ZHU D, ZHAO X et al. HMGA2 promotes vasculogenic mimicry and tumor aggressiveness by upregulating Twist1 in gastric carcinoma. Sci Rep 2017; 7: 2229. https://doi.org/10.1038/s41598-017-02494-6[37]
LIANG L, KANG H, JIA J. HCP5 contributes to cisplatin resistance in gastric cancer through miR-128/HMGA2 axis. Cell Cycle 2021; 20: 1080–1090. https://doi.org/10.1080/15384101.2021.1924948

[38] LIU Z, LÜ Y, JIANG Q, YANG Y, DANG C et al. miR-491 inhibits BGC-823 cell migration via targeting HMGA2. Int J Biol Markers 2019; 34: 364–372. https://doi.org/10.1177/1724600819874488

[39] LI W, LI J, MU H, GUO M, DENG H. MiR-503 suppresses cell proliferation and invasion of gastric cancer by targeting HMGA2 and inactivating WNT signaling pathway. Cancer Cell Int 2019; 19: 164. https://doi.org/10.1186/s12935-019-0875-1

[40] CAI X, NIE J, CHEN L, YU F. Circ_0000267 promotes gastric cancer progression via sponging MiR-503-5p and regulating HMGA2 expression. Mol Genet Genomic Med 2020; 8: e1093. https://doi.org/10.1002/mgg3.1093

[41] XIA Y, LV J, JIANG T, LI B, LI Y et al. CircFAM73A promotes the cancer stem cell-like properties of gastric cancer through the miR-490-3p/HMGA2 positive feedback loop and HNRNPK-mediated β-catenin stabilization. J Exp Clin Cancer Res 2021; 40: 103. https://doi.org/10.1186/s13046-021-01896-9

[42] CHAN CC, DOSTIE J, DIEM MD, FENG W, MANN M et al. eIF4A3 is a novel component of the exon junction complex. RNA 2004; 10: 200–209. https://doi.org/10.1261/rna.5230104

[43] WANG R, ZHANG S, CHEN X, LI N, LI J et al. EIF4A3-induced circular RNA MMP9 (circMMP9) acts as a sponge of miR-124 and promotes glioblastoma multiforme cell tumorigenesis. Mol Cancer 2018; 17: 166. https://doi.org/10.1186/s12943-018-0911-0

[44] CAO C, WU X, LI Z, XIE Y, XU S et al. EIF4A3-Bound hsa_circ_0006847 Exerts a Tumor-Suppressive Role in Gastric Cancer. DNA Cell Biol 2024; 43: 232–244. https://doi.org/10.1089/dna.2023.0397

[45] HOU G, ZUO H, SHI J, DAI D, WANG H et al. EIF4A3 induced circABCA5 promotes the gastric cancer progression by SPI1 mediated IL6/JAK2/STAT3 signaling. Am J Cancer Res 2023; 13: 602–622.

[46] WU Y, ZHAO H. Circ_0074027 binds to EIF4A3 and promotes gastric cancer progression. Oncol Lett 2021; 22: 704. https://doi.org/10.3892/ol.2021.12965

[47] WANG G, SUN D, LI W, XIN Y. CircRNA_100290 promotes GC cell proliferation and invasion via the miR-29b-3p/ITGA11 axis and is regulated by EIF4A3. Cancer Cell Int 2021; 21: 324. https://doi.org/10.1186/s12935-021-01964-2

[48] SUN D, WANG G, XIAO C, XIN Y. Hsa_circ_001988 attenuates GC progression in vitro and in vivo via sponging miR-197-3p. J Cell Physiol 2021; 236: 612–624. https://doi.org/10.1002/jcp.29888

[49] JIANG X, PENG M, LIU Q, PENG Q, OYANG L et al. Circular RNA hsa_circ_0000467 promotes colorectal cancer progression by promoting eIF4A3-mediated c-Myc translation. Mol Cancer 2024; 23: 151. https://doi.org/10.1186/s12943-024-02052-5

https://doi.org/10.4149/neo_2024_240502N196

EIF4A3-induced circle RNA_ 0001860 promotes growth, invasion, and immune evasion of gastric cancer cells through the miR-618/HMGA2 axis

Xiaoyi ZHANG[1], Jiaqi LI[2], Qian ZHANG[2,*]

Supplementary Information

Supplementary Table S1. The sequences used in this study.

Name	Sequences
sh-circ_0001860#1	AACTCTGTTACTGAAGCTTCA
sh-circ_0001860#2	ACTCTGTTACTGAAGCTTCAA
sh-circ_0001860#3	TTACTGAAGCTTCAAGGTTAC
sh-NC	TTCTCCGAACGTGTCACGT
miR-618 mimics	AAACUCUACUUGUCCUUCUGAGU
miR-618 antagomir	ACUCAGAAGGACAAGUAGAGUUU
miR-NC	CAAACTACGGAGTGGACACTCCTCA
Primers for a region	Forward: TGAGCTATAGAACCAGAACCAAGG Reverse: ACAAAACTTAAAGCAGCTCTCAC
Primers for b region	Forward: ACTTAAACTGGCATGATCTGAACT Reverse: ACCTTGAAGCTGCAAAAGAGA
Primers for c region	Forward: TGATGTTTGGTGGCTATGAGACT Reverse: TCCACCTCACTATCAACACTCA
Primers for d region	Forward: GCTGTCAGATGGGTCAGAGG Reverse: ACATCCCAGTAGCATCCAGC